Babaei et al., *BioImpacts.* 2023;13(6):475-487
doi: 10.34172/bi.2023.24266
https://bi.tbzmed.ac.ir/

Enhanced growth and differentiation of neural stem cells on alginate/collagen/reduced graphene oxide composite hydrogel incorporated with lithium chloride

Azadeh Babaei[1], Taki Tiraihi[1*], Jafar Ai[2], Nafiseh Baheiraei[1]

[1]Department of Anatomical Sciences, Faculty of Medical Sciences, Tarbiat Modares University, Tehran, Iran
[2]Department of Tissue Engineering and Applied Cell Sciences, School of Advanced Technologies in Medicine, Tehran University of Medical Sciences, Tehran, Iran

Article Info

Article Type:
Original Article

Article History:
Received: 31 Jan. 2022
Revised: 14 Aug. 2022
Accepted: 16 Aug. 2022
ePublished: 24 July 2023

Keywords:
Spinal cord injury
Alginate
Collagen
Reduced graphene oxide
Injectable hydrogel
Neural stem cell

Abstract

Introduction: Cell transplantation with hydrogel-based carriers is one of the advanced therapeutics for challenging diseases, such as spinal cord injury. Electrically conductive hydrogel has received much attention for its effect on nerve outgrowth and differentiation. Besides, a load of neuroprotective substances, such as lithium chloride can promote the differentiation properties of the hydrogel.

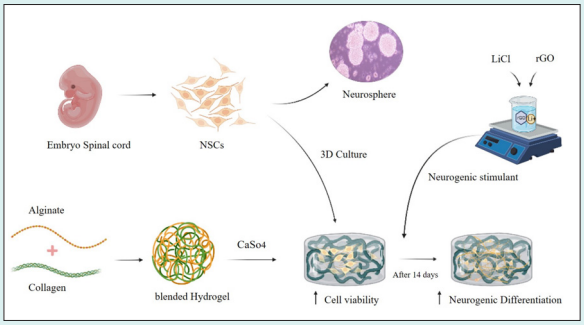

Methods: In this study, alginate/collagen/reduced graphene oxide hydrogel loaded with lithium chloride (AL/CO/rGO Li+) was prepared as an injectable cell delivery system for neural tissue regeneration. After determining the lithium-ion release profile, an MTT assay was performed to check neural viability. In the next step, real-time PCR was performed to evaluate the expression of cell adhesion and neurogenic markers.

Results: Our results showed that the combination of collagen fibers and rGO with alginates increased cell viability and the gene expression of collagen-binding receptor subunits such as integrin α1, and β1. Further, rGO contributed to the controlled release of lithium-ion hydrogel in terms of its plenty of negatively charged functional groups. The continuous culture of NSCs on AL/CO/rGO Li+ hydrogel increased neurogenic genes' expressions of nestin (5.9 fold), *NF200* (36.8 fold), and synaptophysin (13.2 fold), as well as protein expression of *NF200* and synaptophysin after about 14 days.

Conclusion: The simultaneous ability of electrical conduction and lithium-ion release of AL/CO/rGO Li+ hydrogel could provide a favorable microenvironment for NSCs by improving their survival, maintaining cell morphology, and expressing the neural marker. It may be potentially used as a therapeutic approach for stem cell transplantation in a spinal cord injury.

Introduction

Stem cell transplantation is considered a promising strategy in recovery from sensory and motor injuries after spinal cord injury (SCI).[1] Previous studies have described that neural stem cells (NSCs) have a great therapeutic potential in the treatment of SCI.[2-5] Studies have shown that NSCs could be used for the recovery of lost cells and protect the injury site through suppress neuroinflammation.[3,6-8] Many previous studies have reported that transplantation of NSCs into the site of injury promotes remyelination and functional recovery.[2,9-11]

However, the challenge in stem cell transplantation is poor survival of stem cells due to mechanical damage during injection or ischemia of the injured area. Also, issues such as de-differentiation and transplantation rejection can limit the effectiveness of cell transplantation. In this regard, creating a favorable microenvironment for cell transfer can enhance the efficiency of transplantation.[12,13]

Cell delivery in hydrogel ameliorates cell survival and provides a proper environment for cell adhesion,

*Corresponding author: Taki Tiraihi, Email: takialtr@modares.ac.ir

proliferation, and differentiation.[14,15] Furthermore, a hydrogel with the incorporation of growth factors, drugs, and cells can provide a localized controlled delivery system.[16-18]

Alginate is a herbal polysaccharide consisting of carboxylated guluronic and mannuronic acid units with a linear structure similar to hyaluronic acid and could be an attractive option for nerve culture.[19] Alginate does not have cell adhesion properties but can be overcome by chemical manipulation or blending with other cells' adhesive materials.[20-23] Previous studies have also shown that collagen is a suitable candidate to be combined with alginate. It has also been reported that when the cells were cultured in this scaffold, they could enhance the expression of α1, α2, and β1 integrins.[24] Studies have shown that alginate with incorporation of neurotrophic factors is a suitable biomaterial that can stimulate axonal regeneration in SCI.[25-27]

Collagen is an important structural protein in the extracellular matrix (ECM) and it contains integrin-binding sites for cell interaction with matrix.[28] Previous studies have successfully used collagen, in various applications such as reconstruction of tissue defects, wound healing, and nerve regeneration.[29] Collagen could be combined with alginate to improve cell viability as well as proliferation and regeneration.[30]

Considering that the activity of nerve cells is electricity-dependent, the use of electroactive materials such as graphene-based material can provide an advantage substrate for nerve stimulation.[31] It has been found that electrical stimulation of conductive substrates could affect the behavior and fate of the cells.[32,33] Graphene-based materials, especially reduced graphene oxide (rGO), are successfully used in nerve tissue engineering due to their desirable properties such as great electrical conductivity, biocompatibility, and mechanical strength.[34-36] It has been reported that graphene could effectively enhance neuronal cell behavior in terms of neural-specific gene expression and guidance axon growth.[37,38] Furthermore, rGO has a higher surface area and plenty of surface functional groups including carbonyl group and hydroxyl, which can improve the surface capacity to bind with other biomaterials such as drugs and chemical molecules, and facilitate alginate biocompatibility.[39]

Lithium chloride is a small molecule with neuroprotective activity and is utilized as a mood stabilizer in the treatment of bipolar disorder and depression.[40,41] Lithium-ion could induce proliferation as well as neuronal differentiation of cultured hippocampal and spinal cord neural progenitor cells.[42-44] In an animal model, lithium-ion could enhance hippocampal neurogenesis due to reducing the microglia and inflammatory macrophage,[45] and boosting the recovery of an injured spinal cord by brain-derived growth factor.[42,43,46,47]

In this study, the blended hydrogel of alginate, collagen, and rGO loaded with lithium chloride has been developed as an injectable cell delivery system for the repair of the injured spinal cord. The pore structure, swelling, mechanical properties of hydrogel, and releasing efficiency of lithium-ion from it, as well as the growth and differentiation of NSCs in this three-dimensional (3D) hydrogel network, were investigated. The incorporation of rGO, a conductive substrate, and lithium-ion into blended hydrogel could provide a suitable microenvironment for improving neurogenesis and synaptogenesis.

Materials and Methods

Materials

Low molecular weight sodium alginate (LMV), high molecular weight sodium alginate (HMV), and rGO particle and sterilized collagen type I were purchased from Sigma Aldrich (Burlington, United States), and B27 supplements was purchased from Gibco (Cambridge, UK). Primary and Secondary antibodies for immunofluorescence staining were purchased from Abcam (Cambridge, UK). cDNA synthesis kits for RT-PCR were purchased from SMOBIO Technology (Hsinchu, Taiwan). Other chemicals were purchased from Sigma Aldrich.

Hydrogel preparation

According to previous study[48] 1:1 ratio of low molecular weight sodium alginate (LMV) (30 mg/mL) and high molecular weight sodium alginate (HMV) (30 mg/mL) were prepared by dissolving alginate powder in phosphate-buffered saline containing calcium and magnesium ions (PBS++) under constant stirring. The prepared alginate solution was filtered through 0.22 μm nylon membrane. Then an aqueous rGO at a concentration of 20 μg/mL was added to the alginate (AL) solution to create the electroactive hydrogels. Next step, AL/rGO solution were mixed with sterilized collagen (CO) solution (5 mg/mL) at 1:1 ratio to obtain a solution of 10.5 mg/mL alginate and 2.5 mg/mL collagen. It was considered AL and AL/CO solutions as control groups besides the AL/CO/rGO. After preparing the solutions, the injectable potential of three mixtures including AL, AL/CO, and AL/CO/rGO were confirmed by passing through a syringe (30 gauge), at room temperature.

For hydrogel formation, sterilized calcium sulfate slurry (40 μL of CaSO4 per 1 mL of solution) was introduced to the AL and AL/CO and AL/CO/rGO solutions to crosslink the hydrogels. A pilot study was conducted to determine the gelation time for hydrogels. According to that, 25 minutes, 15 minutes, and 10 minutes were required for hydrogel AL, AL/CO, and AL/CO/rGO, respectively.

Hydrogel characterizations

Swelling ratio

To evaluate the swelling ratio of the prepared hydrogels, the samples were lyophilized in a freeze-dryer (Alpha 1-4 LD plus; Martin Christ, Osterode am Harz, Germany),

and incubated at 37°C in PBS solution. The samples were taken out at predetermined time points and weighed after the excess solution was blotted. The equilibrium swelling of each hydrogel was calculated according to the following formula.[49,50] All measurements were done in triplicate.

$$Q\ (\%) = [(W_w - W_d)/\ W_d] \times 100 \quad (1)$$

Q: swelling ratio, W_w: swollen state mass, $W_{d:}$ dried state mass.

Scanning electron microscopy (SEM)

SEM was performed to assess the morphology of the prepared hydrogel. The samples were frozen and freeze-dried, at 0.060 mbar for 24 hours, and were then coated with gold. The hydrogels were examined using SEM (VegaII TESCAN, Brno, Czech) with an accelerating voltage of 15 kV. Finally, Pore sizes were calculated from the SEM images (n=3) using ImageJ software (version. 1.53e).

Rheological analysis

Oscillatory rheology was performed using a rheometer (Physica, MCR 501, Anton Paar, Graz, Australia) equipped with two 50 mm parallel plates. Hydrogels were prepared in cylindrical specimens (25 mm in diameter and 2 mm in thickness). The elastic modulus (G′) and viscous modulus (G″) changes were investigated in frequency sweep tests (0. 01–100 rad/s) and at a strain of 0.3%.[51]

Fourier transform infrared spectroscopy (FTIR)

Chemical characteristics of AL, pure CO, AL/CO and AL/CO/rGO were evaluated using FTIR (PerkinElmer spectrometer, Hamburg, Germany). The spectra were recorded within the range of 550–4000 cm^{-1} with a resolution of 4 cm^{-1} and 32 scans.

Electrical conductivity

The electrical conductivity of freeze-dried hydrogel was measured by a four-point probe instrument (Model 196 System DMM, Keithley, Cleveland, United States). Electrical conductivity was calculated using the following formula. Electrical current was acquired after flowing the voltage.

$$\sigma\ (S / m) = (2.44 \times 10 / S) \times (I / E) \quad (2)$$

σ: conductivity, S: sample side area, I: current through the outer probes, and E: voltage drop across the inner probe.

Lithium-ion release from hydrogels

To prepare lithium chloride loaded hydrogels, three types of AL, AL/CO and AL/CO/rGO solutions were prepared as described above. Lithium chloride was dissolved in polymer solutions before collagen was added, under stirring condition. Next, hydrogels were cast in cylindrical specimens (25 mm in diameter and 2 mm in thickness), incubated in PBS at 37°C. At several time intervals, 1 ml of release medium was withdrawn and replaced with an equal volume of fresh PBS. The amount of drug in the release media was measured using atomic absorption spectrophotometer (PU9100X, Philips, Amsterdam, Netherlands). The cumulative release was obtained according to the following equation. Samples taken from blank hydrogels were used to subtract background readings.[52] FTIR test, as described above, was performed for the final mixture of AL/CO/rGO Li+ hydrogel to evaluate the interaction between the hydrogel and lithium-ion.

$$Q = C_n V_t + V_s \Sigma C_{n-1} \quad (3)$$

Q: cumulative weight of lithium-ion, C_n: lithium-ion concentration at time t, V_t: volume of the release medium, V_s: volume of supernatant in each sampling time.

Isolation, culture, and characterization of NSCs

Under sterile conditions, NSCs were isolated from 13.5-day embryonic mouse spinal cord according to the standard guidelines approved by the Ethics Committee of Tarbiat Modares University. Cells were cultured in a growth medium containing DMEM/F12 medium supplemented with 2% B27, bFGF 20 ng/mL (R&D Systems, United States), EGF 20 ng/mL (R&D Systems, United States), and 1% penicillin/streptomycin.[53] The half of a growth medium was changed every three days. After 7 days, according to the previous studies, neurospheres were dissociated mechanically.[53,54] In brief, the neurospheres with the culture medium were poured into the Falcon and centrifuged. Then, it was resuspended in the culture medium and gently titrated until a creamy suspension was obtained. After 5 minutes, remove the supernatant containing single cells and continue the titration until most of the neurospheres were single. The single cells supernatant was centrifuged for 5 minutes at 1000 rpm, resuspended in fresh growth medium, and cultivated in humidified atmosphere containing 5% CO_2 at 37°C at 37°C. These isolated cells were designated as 'first passage' (P1). All experiments were performed with P1.

To identify NSCs, immunohistochemistry was performed with nestin, SOX2 antibodies according to the standard procedure and visualized using a fluorescence microscope (Olympus IX 53, Tokyo, Japan).[55]

MTT and proliferation assay

The biocompatibility of hydrogels was evaluated. MTT assay was performed following the manufacturer's instructions. Three different culture conditions were compared: The neurospheres were mechanically dissociated into single cells and grown with a density of 1×10^6 cells/mL in (i) AL, (ii) AL/CO, (iii) AL/CO/rGO sterile hydrogel. The cell culture in two-dimensional (2D) was considered as control. The cell viability was assessed at 1, 3, and 7 days post-encapsulation. At each time point, sodium citrate was used to dissolve AL hydrogel and sodium citrate/collagenase was used to dissolve AL/CO and AL/CO/rGO. In brief, after washing the hydrogels

several times, sodium citrate 3% and collagenase (0.5 mg/mL) were added to the hydrogels and incubated for 30-60 minutes until the hydrogels are completely dissolved.[56,57] Then, the cell was exposed to MTT solution and incubated at 37°C for 4 hours. Then, the MTT solution was discarded, whereby DMSO was added. The absorbance was determined using an Elisa microplate reader (Anthos 2020, Biochrom, Cambridge, UK).

Further, DAPI nuclear staining was performed for evaluating the proliferation of encapsulated NSCs in hydrogel. The samples were washed with PBS on days 1,3 and 7 following cell encapsulation. They were then stained with 4', 6- diamidino-2-phenylindole (DAPI) to label nuclei of the cells. The cell fluorescence was photographed using a fluorescence microscope.

Integrin subunit expression and cells attachment

The expression of collagen-binding integrin subunits was examined to evaluate cell adhesion to hydrogel. Total RNA were extracted 24 hours after cell encapsulation in hydrogel. cDNA was synthesized using cDNA Synthesis Kit, and real-time was performed as described below. Primer sequences of integrin subunits α1, β1 are presented in Table 1. Also SEM analysis was performed after they were fixed with glutaraldehyde at 4°C for 1 hour and then dehydrated by ethanol gradient.[58]

Neurogenesis potential of NSC in hydrogel

To evaluate the NSCs differentiation on the AL, AL/CO, AL/CO/rGO, and AL/CO/rGO loaded with lithium chloride (AL/CO/rGO Li+) hydrogel, the neurospheres were mechanically disassociated into single cells and resuspended in sterile hydrogel solution at a density of 1×10^6 cells/mL. The mixture was pipetted into a 48-well plate and incubated at 37°C to form a gel. Once the cells were encapsulated in the three-dimensional hydrogel, cell medium DMEM/F12 containing B27 (2%) and FBS 5% was added to the top of the gels and incubated at 37°C and 5% CO_2 for 14 days. The culture media were changed every 3 days.

Real-time RT-PCR analysis

Total RNA was extracted and cDNA was synthesized using Transcriptor First Strand cDNA Synthesis Kit. The qRT- PCR was performed using SYBR Green master mix (Ampliqon) and an Applied Biosystems 7500 (Life Technologies, California, US) according to the manufacturer's protocol. Method $2^{-\Delta\Delta Ct}$ was used to calculate relative gene expression analysis for hydrogel was compared to the 2D cultured. *GAPDH* was used as the housekeeping gene.[59]

Primer sequences of integrin subunits α1, β1 and nestin, neurofilament 200 (*NF200*) and synaptophysin are presented in Table 1.

Immunofluorescence staining

Cell-laden hydrogels were fixed with 4% paraformaldehyde on day 14 post-encapsulation. Immunofluorescence staining was performed with primary antibodies: anti-*NF200* (1:500, mouse IgG) and anti-synaptophysin (1:500, mouse IgG) at 4°C overnight. Thereafter, they were washed with PBS, incubated with FITC-conjugated secondary antibody at room temperature, and counterstained with DAPI. Immunoreactivity was investigated via fluorescence microscopy.[64] The number of branch points along the neurite was measured using Image J software.

Statistical analyses

The data were presented as the mean ± standard deviation. All quantitative experiments were analyzed using one-way or two-way analysis of variance (ANOVA) and Tukey multi-comparison tests using GraphPad Prism (Version 8.4.0; GraphPad Software). A P value of <0.05 was considered statistically significant.

Results

Construction and characterization of hydrogel

AL/CO/rGO hydrogels were ironically crosslinked to generate hybrid hydrogels, with (Fig. 1 A-C) displaying the optical photo of the three group hydrogels. As can be seen, all hydrogels have been uniform, and the color

Table 1. Forward and reverse sequences of primers used in qRT-PCR

Gene	Sequences of forward and reverse primers	Fragment size (bp)	Reference
Integrin α1	CACCTTTCAAACTGAGCCCGCCA GCTGCCCAGCGATGTAGAGCACAT	110	60
Integrin β1	TCTCACCAAAGTAGAAAGCAGGGA ACGATAGCTTCATTGTTGCCATTC	138	60
Nestin	CACACCTCAAGATGTCCC GAAAGCCAAGAGAAGCCT	114	61
NF200	AGTACCAGGACCTGCTCAAC GTGAGTGGACATGGAGGGAA	155	62
Synaptophysin	AGCCTCCTCCACTCAGTCTA GCATTCCTCAGCCCCTATCT	243	62
GAPDH	AAGTTCAACGGCACAGTCAAGG CATACTCAGCACCAGCATCACC	121	63

qRT-PCR: Quantitative Reverse Transcription PCR

of hydrogels was noticed to be darker following the incorporation of rGO. In all hydrogels, injectability was initially confirmed via a 30-gauge needle (data not shown). The addition of collagen and rGO accelerates the gelation of the AL hydrogel, so that the hydrogel turns into a gel within 10 minutes, and this is the suitable time to use it for in situ injection.

The SEM electron micrograph (Fig. 1D-F) reveals the porous structures of these hydrogels. They displayed high porosity which became dense upon incorporation with the collagen and rGO. As shown in the graph (Fig. 1G), the average pore diameters were 197.73 ± 26.34, 155.71 ± 30.67, and 141.24 ± 10.13 μm in AL, AL/CO and AL/CO/rGO hydrogels, respectively. The statistical difference was significant between AL and AL/CO/rGO.

The results of the swelling ratio and water content of hydrogels are shown in Fig. 1H; the swelling ratios of hydrogels revealed an ascending trend in the first 200 minutes after immersion in PBS. In periods longer than 200 minutes, it reached a plateau which can show the state of equilibrium of absorption. Finally, the corresponding amount of water content for AL, AL/CO, and AL/CO/rGO was 87.41 ± 2.45, 78.92 ± 0.98, and 73.48 ± 0.52, respectively. Collagen and rGO incorporation in AL resulted in relatively lower swelling ratios. The endpoints of the study (250 minutes) were statistically significant among the hydrogels, while at the other time points, the level of significance was variable.

Rheological properties of the hydrogels (Fig. 1I) were detected by measuring the storage modulus (G′) and loss modulus (G″); the AL/CO/rGO hydrogel presented more than 57 and 118 times increase in the storage modulus compared to AL and AL/CO at a frequency of 1 rad/s, respectively. Revealed that the presence of rGO results in an increase in the gel stiffness.

The results obtained from the electrical conductivity revealed AL hydrogel alone had a conductivity of about $5.3\times10^{-8} \pm 0.04$ S/m, which is considered a non-conductive material and by adding rGO, the conductivity grew to about $8.6\times10^{-4} \pm 0.21$ S/m.

Lithium-ion release from hydrogels

The cumulative release behavior was investigated with the results presented in Fig. 2A. As shown, an initial burst release within 24 hours after is seen in all three hydrogels. While in the rGO-containing group, the burst is reduced to 17.6% and followed almost sustain continues up to 15 days when about 73.67% of drug was released. On the other hand, in the AL/CO and AL/CO/rGO groups, 39.08% and 53.73% of initial burst release were measured

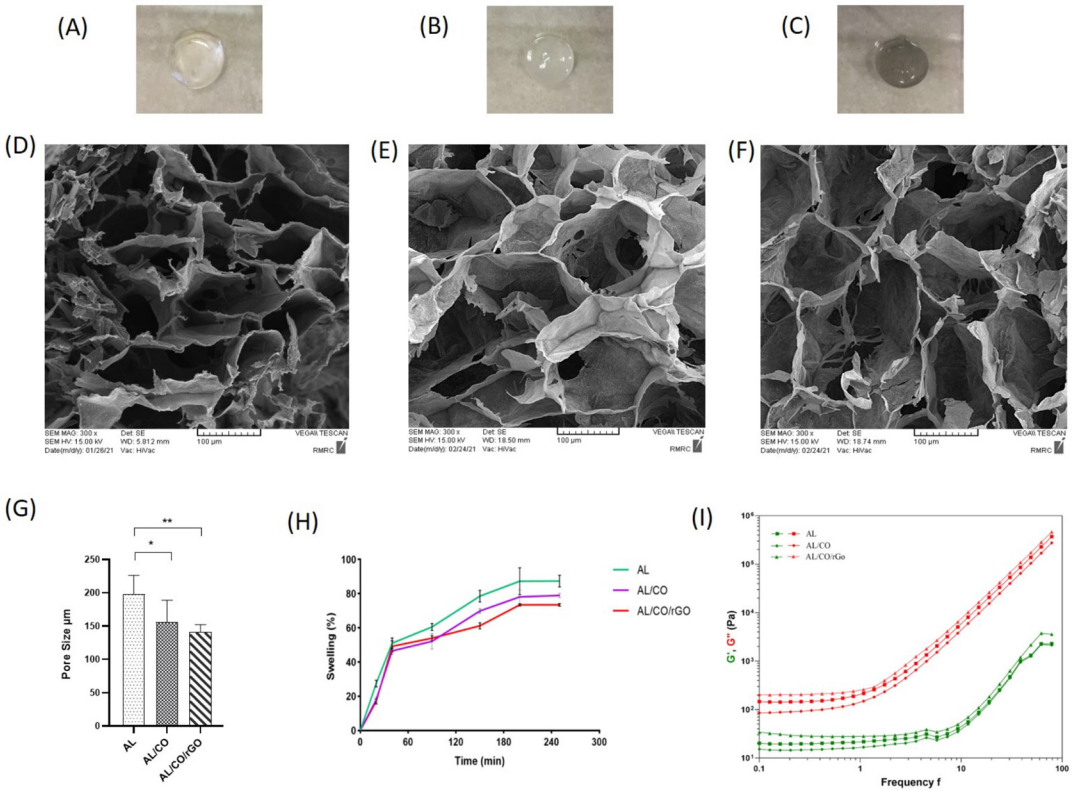

Fig. 1. Hydrogel fabrication and characterization. The photographs of hydrogel groups which were used in the experimental design (A-C) AL, AL/CO, and AL/CO/rGO hydrogel, respectively. SEM image of prepared hydrogel showing porous structure, (D-F) AL, AL/CO and AL/CO/rGO hydrogel, respectively. (G) The pore sizes of the hydrogel networks decreased with incorporation of collagen and rGO content (* $P < 0.05$, ** $P < 0.01$ / n = 3). (H) Swelling ratio of prepared hydrogels were indicated in 250 min (n = 3). (I) Rheological characterization of AL, AL/CO, and AL/CO/rGO hydrogels (n = 3). AL: Alginate hydrogel; AL/CO: alginate/collagen hydrogel; AL/CO/rGO: alginate/collagen/reduced graphene oxide hydrogel.

in the first 24 hours, respectively. Also, in AL and AL/CO groups, 83.76% and 87.21% of the drug were released after two weeks, respectively.

Fourier transform infrared spectroscopy

Fig. 2B shows the FTIR spectra of the AL, pure CO, AL/CO, AL/CO/rGO, and AL/CO/rGO Li+ mixture. IR spectrum of AL shows carboxyl (symmetric COO stretching vibration) and hydroxyl groups at 1619 cm^{-1} and 3424 cm^{-1} respectively.[65] In the IR spectra of pure CO, the N–H stretching vibration peak for amide A was 3399 cm^{-1}, and an amide I band (1618 cm^{-1}), amide II bands (1547 cm^{-1}), and C=O band (1695 cm^{-1}) were evident.[66] The IR spectra of the AL/CO combination showed merged peaks, indicating that the components were properly combined to create the desired hydrogel.[67] The peaks in the AL/CO/rGO hydrogel overlap because of the shared functional groups COO and OH in the rGO and AL/CO structures. The oxygen functional groups such as OH and COO on the GO surface create hydrogen bonds with the molecular chains of the AL, which can increase adhesion between the rGO and AL surfaces.[68] In the spectrum related to AL/CO/rGO Li+, absorption peaks related to OH, CO and COO bonds, have shifted. It can indicate the electrostatic interaction between Lithium-ion and OH, CO and COO functional groups on the rGO surface.[69]

Culture and identification of NSCs

Stem cells were isolated from the E13.5 fetal mouse spinal cord, about 4 days after culture in growth medium. Some of the stem cells proliferated into floating spherical cluster with a roughly uniform size and typical shape called neurosphere (Fig. 3A, B). The neurospheres were passaged using mechanical dissociation after 7 days (Fig. 3C, D). The neurospheres were stained positive for NSCs markers including nestin (green fluorescence) and SOX2 (green fluorescence) (Fig. 3E, F).

Biocompatibility and proliferation assay

To further confirm hydrogel cytocompatibility, the MTT assay was performed using NSCs (Fig. 4A). The AL/CO/rGO groups revealed a significantly higher absorbance value of cell compared to the control group at 3 and 7 days post-incubation (**P <0.01, **P < 0.01 respectively). However, on the first day, no significant difference was observed between the groups, possibly because of cell adaption. In addition, the AL/CO group had a significant increase in absorption value after 3 and 7 days (*P < 0.05, **P < 0.01, respectively), compared to the control group. Such results indicate AL/CO and AL/CO/rGO hydrogel had good cytocompatibility of compared to 2D, AL groups.

To visualize the capacity of the proliferation of encapsulated stem cells on different hydrogels, DAPI staining via fluorescent microscopy was used on 1, 3, and 7 days post-cultivation. As depicted in Fig. 4D-F, no significant change was observed one day after cell encapsulation, but an obvious proliferation in cells was observed in AL/CO (Fig. 4G-I) and AL/CO/rGO (Fig. 4 J-L) hydrogel groups compared to the Al groups on days 3 and 7.

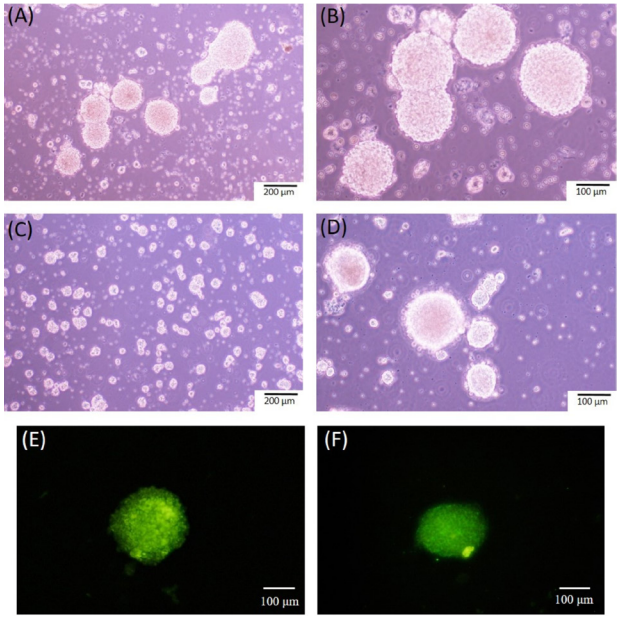

Fig. 3. Culture and characteristics of NSCs. (A-B) Neurospheres showing spherical uniform size on day 4 and (C-D) after the first passage. (E) Fluorescence staining of neurospheres indicating nestin and (F) SOX2 expression.

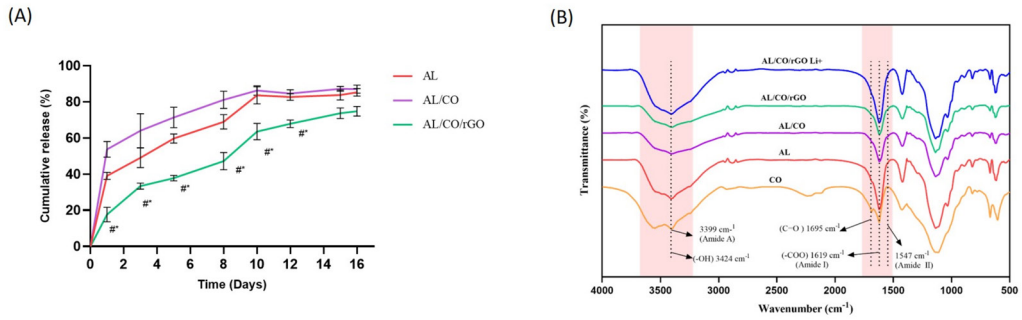

Fig. 2. Drug release profile and FTIR absorbance. (A) Drug release profile of AL, AL/CO, and AL/CO/rGO hydrogels loaded with lithium chloride, (n = 3). (B) FTIR spectra of AL, pure CO, AL/CO, AL/CO/rGO, and AL/CO/rGO Li+ hydrogel (n = 3).

Cell adhesion and Integrin expression of NSCs in hydrogel

The gene expression of integrin subunits (α1, β1) which are responsible for identifying and binding the matrix collagen,[70] was evaluated after 24 hours by real-time PCR (Fig. 4B). Both α1 and β1 integrin subunits significantly enhanced with mean fold changes by 1.75, 2.9 times in the AL/CO group 24 hours after cell encapsulation compared to the AL group, respectively. Further, with the addition of rGO the expression of α1 and β1 integrin subunits increased with mean fold changes of 2.45, and 4.05 times, respectively. Furthermore, the morphology of cells encapsulated in AL/CO/rGO hydrogels was investigated by SEM. As seen in (Fig. 4C), the hydrogels could support cell adhesion and improve cell spreading.

Differentiation of encapsulated cells in hydrogel

For considering the neuronal differentiation tendency of NSCs cultured in on the AL, AL/CO, AL/CO/rGO and AL/CO/rGO Li+, the genes expression levels of neuronal-specific makers were assessed on day 14. The expression of neural markers such as nestin, *NF200*, and synaptophysin was assessed in all above groups. The gene expression of NSCs in the two-dimensional (2D) was considered as control. According to the results, (Fig. 5A), the gene expression of nestin in AL/CO, AL/CO/rGO, and AL/CO/rGO Li+ group significantly increased compared with the control 2D group (**P < 0.01, ***P < 0.001, ***P < 0.001 respectively). The expression level of nestin in AL/CO increased by 2.5 times (**P < 0.01). Also, in AL/CO/rGO, nestin showed significantly enhanced expression (**P < 0.01).

As indicated (Fig. 5B), the mRNA expression level of *NF200* was significantly highest in both AL/CO/rGO and AL/CO/rGO loaded with lithium-ion (AL/CO/rGO Li+) groups (***P < 0.001). Note that *NF200* expression in AL/CO/rGO was significantly higher than in AL/CO groups (***P < 0.001). Also, AL/CO/rGO Li+ showed a significant increase in *NF200* expression compared with AL/CO/rGO group (**P < 0.01). The expression of synaptophysin (Fig. 5C) was the highest in AL/CO/rGO and AL/CO/rGO Li+ groups, while the AL/CO/rGO Li+ groups showed 3-fold increase in the gene expression compared with AL/CO/rGO. The results showed that the AL/CO/rGO Li+ group compared to 2D culture presented higher expression of neural cell marker in 3D culture compared with 2D control culture on day 14.

The differentiated cells were also immunoreactive to *NF200* and synaptophysin on day 14; the *NF200* immunoreactivity was detectable in all hydrogel groups. Neurons grown in collagen-containing hydrogels seemed

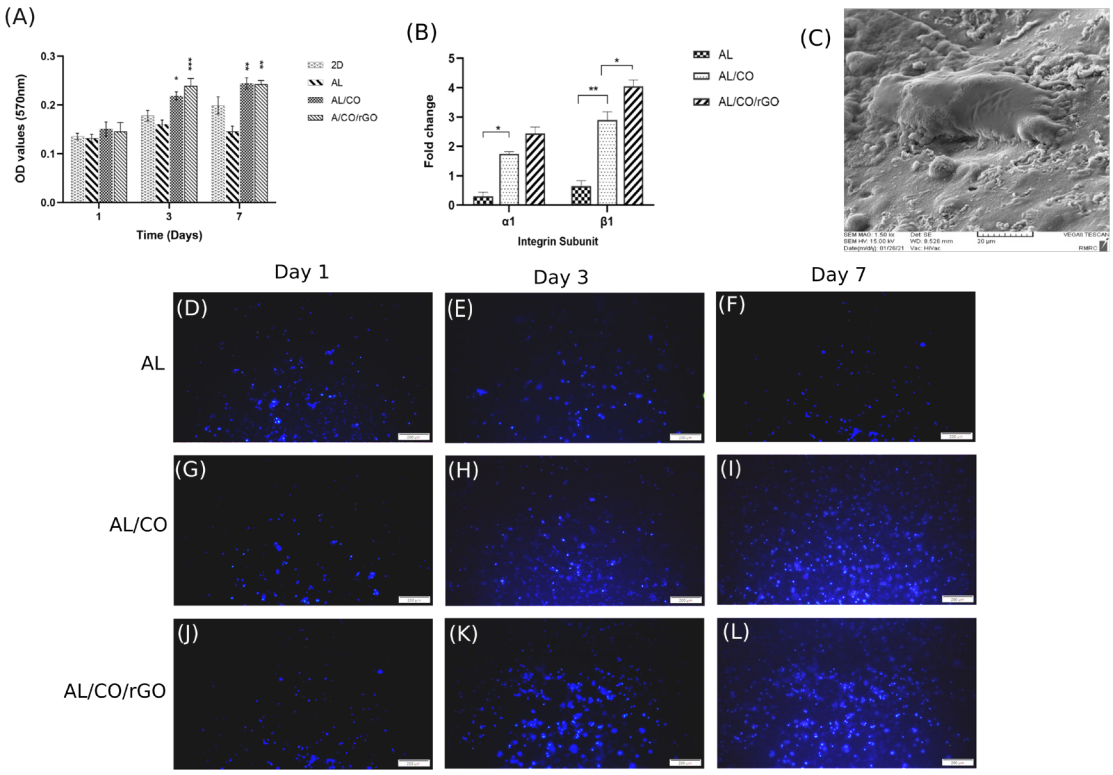

Fig. 4. Cytotoxicity and proliferation assay of NSCs in 3D culture. (A) MTT assay of NSCs on 1,3 and 7 days post encapsulation in hydrogel compared with 2D culture. There was a significant increase in proliferation on day 3 and 7 in AL/CO and AL/CO/rGO (* P < 0.05, ** P < 0.01, *** P < 0.001/ n = 3). (B) Expression of collagen-binding integrin subunits 24 h post-encapsulation in AL, AL/CO, and AL/CO/rGO hydrogels. (C) The SEM image showed the morphology of the encapsulated NSCs inside the AL/CO/rGO hydrogel after 24 hours. (D-F) Investigation of growth rate by DAPI staining of NSCs after 1, 3, and 7 days in 3D culture in (D-F) AL hydrogel, (G-I) AL/CO and (J-L) AL/CO/rGO hydrogels, which showed observable increase in AL/CO and AL/CO/rGO hydrogels on day 4 (n = 3).

to interact with the collagen fibrils and exhibited a neuronal phenotype (FIG. 5H, 5L, 5P). In the group without collagen fibers, the encapsulated cell was unable to form neurite and exhibited spherical shape (Fig. 5D). Synaptophysin (Fig. 5I, 5M, 5Q) in the blend hydrogel was found within the soma of the neurons, while the neurites were few. However, in AL group (Fig. 5E), the immunoreactivity of synaptophysin was inconspicuous and located in soma of the neurons.

As seen in (Fig. 5T), the average length of neurites in the AL/CO/rGO Li + group, about 103.3 ± 15.37, was longer than in the AL/CO/rGO group, about 67.72 ± 9.11 (*$P < 0.05$). This also suggests one of the important factors of neurological maturity. This, together with gene expression data, suggests that cells encapsulated in AL/CO/ rGO Li + matured more efficiently than other groups.

Discussion

The survival and differentiation of transplanted NSCs is a crucial factor in the success of cell therapy.[71] Cell delivery with hydrogel would enhance the efficiency of cell transplantation. Hydrogels can provide a supportive environment for the cell, as well as chemical and physical stimuli with enhancement of cells survival and differentiation, bridge nerve regeneration, and prevent scar formation.[72]

The alginates and collagen mixture provides a heterogeneous network that accelerates NSCs attachment and neural differentiation.[24] The formation of hydrogel under natural conditions also promotes cell survival and facilitates its use in situ delivery.

Recently, conductive substrates such as graphene-based composites have attracted plenty of attention in nerve tissue engineering, in order to ameliorate the transmission of electrical signals in neurons and provide a suitable environment for neuronal regeneration.[73] The high conductivity and special topographic properties of graphene can enhance cell scaffold interactions,[74] electrical stimulation can significantly improve the growth of neurite and nerve regeneration.[75,76] In this study, rGO combined with AL/CO hydrogel was used which can be injected at the site of injury and provides mechanical

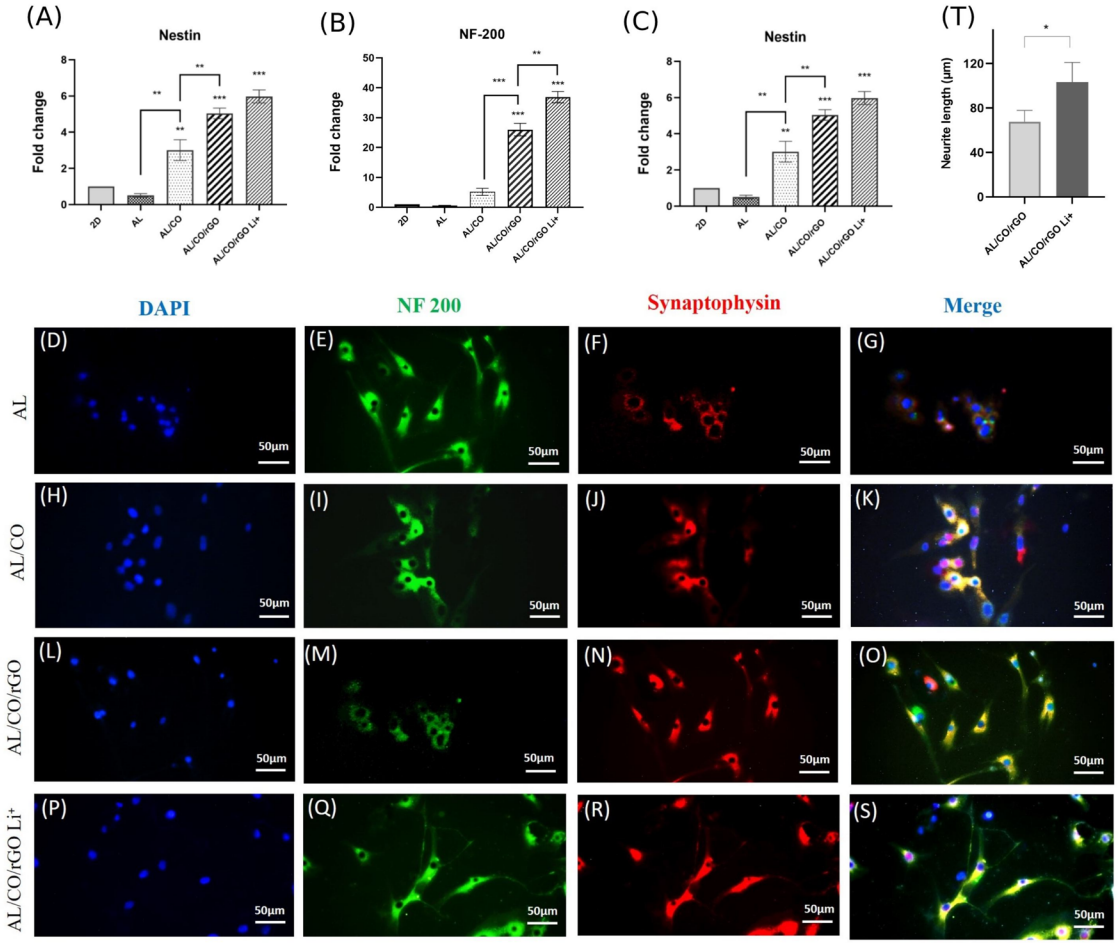

Fig. 5. Gene and protein expression of cultured NSCs in the hydrogel. mRNA expression of (A) Nestin, (B) *NF200* and (C) Synaptophyoin after 14 days of neural stem cells culturing on the AL, AL/CO, AL/CO/rGO, and AL/CO/rGO loaded with Lithium-ion compared to 2D culture. (** $P < 0.01$, *** $P < 0.001$, n = 3). Immunocytochemistry of *NF200* and synaptophysin after 14 days cultured on (D-G) Al, (H-K) AL/CO, (L-O) AL/CO/rGO and (P-S) AL/CO/rGO Li+ (n = 3). Cell nuclei were stained with DAPI (blue). (T) The average neurite length of NSCs-derived neurons cultured after 14 days in AL/CO/rGO and AL/CO/rGO Li+ hydrogels. (* $P < 0.01$).

as well as chemical stimuli to direct cell programming towards more efficient differentiation. Further, in situ-gelling system has a great clinical advantage such as ease of administration and being *minimally invasive* which can be considered as one of the best drug delivery systems.[77]

The combination of high and low molecular weight alginate polymer results in increase minimally the viscosity of the solution while the elasticity modulus increases sufficiently. This advantage not only makes syringe injection possible, but it also increases the stability of hydrogel.[78] Williams PA et al. showed that the use of variable molecular weights of alginate improves the controlled release of lipid vesicles by increasing the strength and stability of the hydrogel structure.[48]

Previous studies showed that neurons in a substrate with mechanical properties in the range of nerve tissue generate more branching. Balgude AP et al. showed when the stiffness of agarose gel increases, the extension of neurites decreases.[79] The elastic model in the range of 50–350 is appropriate for nerve tissue, according to research by Flanagan LA et al. The density of branches diminishes as the stiffness increases.[80] In this study, the addition of rGO has reinforced the mechanical properties, although the elastic modulus of all three hydrogels were still in the range of 80-200 Pa in 1 rad/s frequency, especially elastic modules of AL/CO/rGO was 203 Pa, which stiffness was near to the human spinal cord tissue ~200.[81]

It was observed that all three scaffolds had a high swelling rate due to the high porosity and the connection between the pores, which was observed in the SEM image. However, the addition of rGO slightly reduced the pore size. Pore size is involved in cell infiltration, tissue ingrowth, nutrient diffusion, and metabolic waste removal. As such, the optimal pore size according to the target tissue is important; if the pores are too large, it would restrict cell attachment due to a reduction in specific surface area, and if it is too small it would limit cell migration to the center.[82] Previous studies have demonstrated that pore size diameter around 100 um seems to be more proper for the differentiation and regeneration of neurons.[83-85] The addition of rGO boosted the conductivity of hydrogels in limited semiconductor materials. It was reported that conductive substrates were in the range of about 10^{-4} S cm and above affecting the differentiation of stem cells into neurons.[86]

This study showed that rGO could provide electrostatic interaction with lithium-ion through hydroxyl, carbonyl, and carboxyl functional groups. Although alginate also has negatively charged groups in its chemical structure, it is not enough to release lithium-ion in control. While unique chemical structure of rGO has a high surface area with multiple oxygenated functional groups, that it has been able to control the release of lithium-ion and increase the therapeutic benefit of hydrogel through the neuroprotective effect of lithium-ion.[87] However, in the AL/CO/rGO group, a minor initial burst release was considered on the first day. This behavior can be due to accumulation of drugs on the surface of the hydrogel which could be rapidly released into the environment. Related studies reported that GO could be used as immobilization anchor for BMP_2 encapsulated in bovine serum albumin nanoparticles (NPs). They demonstrated that positive charges of the NPs and negative charges of GO could be bound together through electrostatic interaction and provide sustained release of BMP_2.[88]

This study showed that the culture of NSCs in the AL/CO and AL/CO/rGO hydrogel was biocompatible and sufficiently improved cell proliferation compared to control. Rahman et al. reported that the metabolic activity of cells in the gelatin-methacryloyl (GELMA) loaded with GO group increased compared to the GELMA group free GO.[89]

In this study, it was shown that cell survival and proliferation increased upon adding collagen. According to the increased expression of integrin subunits after 24 hours in the AL/CO group, it seems that collagen fibers have been dispersed in the alginate matrix and the cells have been able to interact with the collagen fibers enhancing cell survival and proliferation. In addition, the presence of rGO has been effective in regulating the expression of integrin subunits genes. The effect of graphene-based material on regulating gene expression can be due to the improvement of cell interaction with ECM, which occurs in response to the uptake of protein serum on the scaffold. Previous study has reported that conductive substrates could improve the cell-ECM interaction, which occurs because of the uptake of proteins serum on the scaffold.[74]

Gene expression results of neural markers after 14 days' culture in three-dimensional (3D) hydrogel revealed that the level expression in the three-dimensional group increased compared to the two-dimensional group. In similar studies, encapsulated iPSC-derived neurons in blended alginate and collagen hydrogel made neural networks and matured.[24] The presence of rGO, enhanced the ability of NSCs to differentiate by upregulated gene expression of neuron-specific genes such as nestin, *NF200*, and synaptophysin. These data are in accordance with the data reported by Guo et al. stating that presence the rGO as a coating layer on porcine acellular dermal matrix significantly enhanced neural differentiation of MSCs and regulated gene expression of the nestin, Tuj_1, and MAP_2 protein.[38] In another study, human NSCs cells were cultured on a graphene-cellulose scaffold. They found that the MAP_2 and synaptophysin were expressed only in the GO-containing group.[76]

The effect of conductive substrates in regulating gene expression can be due to the improvement of cell interaction with ECM, which occurs in response to the uptake of protein serum on the scaffold. Indeed, this improvement in cell-ECM interaction stimulates the cellular signaling cascade, thereby affecting gene expression and cellular behavior.[90] In addition, electrical stimulation improves

Research Highlights

What is the current knowledge?

√ Hydrogels as a supportive substrate could be used for the cell and neuroprotective agent delivery in SCI treatment.

√ Electroconductive materials especially rGO are successfully used in nerve tissue engineering.

√ Lithium-ion could affect the proliferation and differentiation of NSCs.

What is new here?

√ rGO improves the controlled release of lithium-ion from the hydrogel.

√ The hydrogel's simultaneous capacity for electrical conduction and lithium-ion release creates an ideal milieu that promotes the expression of neurogenic genes and the growth of neural networks.

cell-cell interactions plus biosignaling transmission and affects the cell fate and behavior.[32,91]

Furthermore, our results confirm the neurogenic effect of lithium chloride with the augmented *NF200* and synaptophysin expression at both mRNA and protein levels. It also showed longer branches of neurites in this group compared to the AL/CO/rGO group suggesting that cells encapsulated in AL/CO /rGO Li+ matured more efficiently than in other groups. In this regard, it was observed that neurons isolated from the fetal hippocampus increased the number of synapses connection after being treated with lithium-ion.[92] Previous studies revealed that lithium chloride improved mesenchymal stem cell survival in the long run and could enhance proliferation or differentiation into neurons in a dose-dependent manner.[93]

Possibly, BDNF signaling pathways might be implicated in the neurogenesis of neural progenitor cells by lithium-ion.[47] Lithium-ion has similar effects as conventional neurotrophins and growth factors in neurogenesis, probably due to activation of the ERK pathway and improvement of neuronal differentiation.[42] Taken together, in this study, injectable electroactive hydrogels were designed and loaded by a neuroprotective agent, lithium chloride, for facilitating neuronal differentiation, which can be applied in SCI regeneration.

Conclusion

This study provided an injectable conductive hydrogel system that may be potentially used in the future for delivering cell and neuroprotective agents such as lithium chloride. The results revealed that AL/CO/rGO Li+ will be effective in creating a microenvironment for transplanted cells to survive and differentiate. The presence of rGO could reinforce the electrical signal and lithium-ion release from hydrogel with neuroprotective activities successfully accelerating the regulation of neuronal differentiation genes and neural network formation in the hydrogel. Nevertheless, animal studies are required to further evaluate its safety and effectiveness for clinical applications.

Acknowledgments

We would like to express our gratitude to the tissue engineering laboratory for the Department of Chemical Engineering, Faculty of Chemical Engineering, Tarbiat Modares University for their help.

Authors' contribution

Conceptualization: Azadeh Babaei, Taki Tiraihi.
Data curation: Azadeh Babaei, Taki Tiraihi, Jajar Ai, Nafiseh Baheiraei.
Formal analysis: Azadeh Babaei, Nafiseh Baheiraei.
Funding acquisition: Taki Tiraihi, Jajar Ai.
Investigation: Azadeh Babaei, Taki Tiraihi, Nafiseh Baheiraei.
Methodology: Azadeh Babaei, Taki Tiraihi, Nafiseh Baheiraei.
Project administration: Taki Tiraihi, Jajar Ai.
Resources: Azadeh Babaei, Taki Tiraihi.
Supervision: Taki Tiraihi, Jajar Ai.
Validation: Azadeh Babaei, Taki Tiraihi, Jajar Ai, Nafiseh Baheiraei.
Visualization: Azadeh Babaei, Taki Tiraihi, Jajar Ai.
Writing–original draft: Azadeh Babaei, Nafiseh Baheiraei.
Writing–review editing: Azadeh Babaei, Nafiseh Baheiraei.

Competing Interests

The authors declare no potential conflicts of interest.

Ethical Statement

This study was approved by the Ethics Committee of the Tarbiat Modares University (Ethics code: IR.TMU. REC.1397.158)

Funding

This research was funded as part of a doctoral thesis in Faculty of Medical Sciences, Tarbiat Modares University, Tehran, Iran (grant number: MED-76968).

References

1. Wyatt LA, Keirstead HSJPibr. Stem cell-based treatments for spinal cord injury. *J Spinal Cord Med* **2012**; 201: 233-52. https://doi.org/10.1016/B978-0-444-59544-7.00012-3
2. Okano H. Stem cell biology of the central nervous system. *J Neurosci Res* **2002**; 69: 698-707. https://doi.org/10.1002/jnr.10343
3. Parr AM, Kulbatski I, Tator CH. Transplantation of adult rat spinal cord stem/progenitor cells for spinal cord injury. *J Neurotrauma* **2007**; 24: 835-45. https://doi.org/10.1089/neu.2006.3771
4. Bonner JF, Connors TM, Silverman WF, Kowalski DP, Lemay MA, Fischer I. Grafted neural progenitors integrate and restore synaptic connectivity across the injured spinal cord. *J Neurosci* **2011**; 31: 4675-86. https://doi.org/10.1523/JNEUROSCI.4130-10.2011
5. Bamber NI, Li H, Aebischer P, Xu XM. Fetal spinal cord tissue in mini-guidance channels promotes longitudinal axonal growth after grafting into hemisected adult rat spinal cords. *Neural Plast* **1999**; 6: 103-21. https://doi.org/10.1155/NP.1999.103
6. Ratajczak MZ, Jadczyk T, Pedziwiatr D, Wojakowski W. New advances in stem cell research: practical implications for regenerative medicine. *Pol Arch Med Wewn* **2014**; 124: 417-26. https://doi.org/10.20452/pamw.2355
7. Cheng Z, Zhu W, Cao K, Wu F, Li J, Wang G, *et al.* Anti-inflammatory mechanism of neural stem cell transplantation in spinal cord injury. *Int J Mol Sci* **2016**; 17: 1380. https://doi.org/10.3390/ijms17091380
8. Rong Y, Liu W, Wang J, Fan J, Luo Y, Li L, *et al.* Neural stem cell-derived small extracellular vesicles attenuate apoptosis and neuroinflammation after traumatic spinal cord injury by activating autophagy. *Cell Death Dis* **2019**; 10: 1-18. https://doi.org/10.1038/s41419-019-1571-8

9. Mitsui T, Shumsky JS, Lepore AC, Murray M, Fischer I. Transplantation of neuronal and glial restricted precursors into contused spinal cord improves bladder and motor functions, decreases thermal hypersensitivity, and modifies intraspinal circuitry. *J Neurosci* **2005**; 25: 9624-36. https://doi.org/10.1523/JNEUROSCI.2175-05.2005
10. Ogawa Y, Sawamoto K, Miyata T, Miyao S, Watanabe M, Nakamura M, *et al.* Transplantation of in vitro-expanded fetal neural progenitor cells results in neurogenesis and functional recovery after spinal cord contusion injury in adult rats. *J Neurosci Res* **2002**; 69: 925-33. https://doi.org/10.1002/jnr.10341
11. Karimi-Abdolrezaee S, Eftekharpour E, Wang J, Morshead CM, Fehlings MG. Delayed transplantation of adult neural precursor cells promotes remyelination and functional neurological recovery after spinal cord injury. *J Neurosci* **2006**; 26: 3377-89. https://doi.org/10.1523/JNEUROSCI.4184-05.2006
12. Rubio D, Garcia-Castro J, Martín MC, de la Fuente R, Cigudosa JC, Lloyd AC, *et al.* Spontaneous human adult stem cell transformation. *Cancer Res* **2005**; 65: 3035-9. https://doi.org/10.1158/0008-5472.CAN-04-4194
13. Jeong J-O, Han JW, Kim J-M, Cho H-J, Park C, Lee N, *et al.* Malignant tumor formation after transplantation of short-term cultured bone marrow mesenchymal stem cells in experimental myocardial infarction and diabetic neuropathy. *Circ Res* **2011**; 108: 1340-7. https://doi.org/10.1161/CIRCRESAHA.110.239848
14. Jhon MS, Andrade JD. Water and hydrogels. *J Biomed Mater Res* **1973**; 7: 509-22. https://doi.org/10.1002/jbm.820070604
15. Assunção-Silva RC, Gomes ED, Sousa N, Silva NA, Salgado AJ. Hydrogels and cell based therapies in spinal cord injury regeneration. *Stem Cells Int* **2015**; 2015: 948040. https://doi.org/10.1155/2015/948040
16. Garbayo E, Montero-Menei C, Ansorena E, Lanciego JL, Aymerich MS, Blanco-Prieto MJ. Effective GDNF brain delivery using microspheres—a promising strategy for Parkinson's disease. *J Control Release* **2009**; 135: 119-26. https://doi.org/10.1016/j.jconrel.2008.12.010
17. Wang Y-C, Wu Y-T, Huang H-Y, Lin H-I, Lo L-W, Tzeng S-F, *et al.* Sustained intraspinal delivery of neurotrophic factor encapsulated in biodegradable nanoparticles following contusive spinal cord injury. *Biomaterials* **2008**; 29: 4546-53. https://doi.org/10.1016/j.biomaterials.2008.07.050
18. Tønnesen HH, Karlsen J. Alginate in drug delivery systems. *Drug Dev Ind Pharm* **2002**; 28: 621-30. https://doi.org/10.1081/DDC-120003853
19. Lee KY, Mooney DJ. Alginate: properties and biomedical applications. *Prog Polym Sci* **2012**; 37: 106-26. https://doi.org/10.1016/j.progpolymsci.2011.06.003
20. Kuo Y-C, Wang C-C. Guided differentiation of induced pluripotent stem cells into neuronal lineage in alginate–chitosan–gelatin hydrogels with surface neuron growth factor. *Colloids Surf B Biointerfaces* **2013**; 104: 194-9. https://doi.org/10.1016/j.colsurfb.2013.01.001
21. Bozza A, Coates EE, Incitti T, Ferlin KM, Messina A, Menna E, *et al.* Neural differentiation of pluripotent cells in 3D alginate-based cultures. *Biomaterials* **2014**; 35: 4636-45. https://doi.org/10.1016/j.biomaterials.2014.02.039
22. Frampton J, Hynd M, Shuler M, Shain W. Fabrication and optimization of alginate hydrogel constructs for use in 3D neural cell culture. *Biomed Mater* **2011**; 6: 015002. https://doi.org/10.1088/1748-6041/6/1/015002
23. Prang P, Müller R, Eljaouhari A, Heckmann K, Kunz W, Weber T, *et al.* The promotion of oriented axonal regrowth in the injured spinal cord by alginate-based anisotropic capillary hydrogels. *Biomaterials* **2006**; 27: 3560-9. https://doi.org/10.1016/j.biomaterials.2006.01.053
24. Moxon SR, Corbett NJ, Fisher K, Potjewyd G, Domingos M, Hooper NMJMS, *et al.* Blended alginate/collagen hydrogels promote neurogenesis and neuronal maturation. *Mater Sci Eng C Mater Biol Appl* **2019**; 104: 109904. https://doi.org/10.1016/j.msec.2019.109904
25. Grulova I, Slovinska L, Blaško J, Devaux S, Wisztorski M, Salzet M, *et al.* Delivery of alginate scaffold releasing two trophic factors for spinal cord injury repair. *Sci Rep* **2015**; 5: 1-19. https://doi.org/10.1038/srep13702
26. Liu S, Sandner B, Schackel T, Nicholson L, Chtarto A, Tenenbaum L, *et al.* Regulated viral BDNF delivery in combination with Schwann cells promotes axonal regeneration through capillary alginate hydrogels after spinal cord injury. *Acta Biomater* **2017**; 60: 167-80. https://doi.org/10.1016/j.actbio.2017.07.024
27. McKay CA, Pomrenke RD, McLane JS, Schaub NJ, DeSimone EK, Ligon LA, *et al.* An injectable, calcium responsive composite hydrogel for the treatment of acute spinal cord injury. *ACS Appl Mater Interfaces* **2014**; 6: 1424-38. https://doi.org/10.1021/am4027423
28. Gorgieva S, Kokol V. Collagen-vs. gelatine-based biomaterials and their biocompatibility: review and perspectives. In: *Biomaterials applications for nanomedicine.* IntechOpen; **2011**. p. 17-52. https://doi.org/10.5772/24118
29. Lee CH, Singla A, Lee Y. Biomedical applications of collagen. *Int J Pharm* **2001**; 221: 1-22. https://doi.org/10.1016/s0378-5173(01)00691-3
30. Baniasadi M, Minary-Jolandan M. Alginate-collagen fibril composite hydrogel. *Materials* **2015**; 8: 799-814. https://doi.org/10.3390/ma8020799
31. Akhavan O, Ghaderi E, Abouei E, Hatamie S, Ghasemi EJC. Accelerated differentiation of neural stem cells into neurons on ginseng-reduced graphene oxide sheets. *Carbon* **2014**; 66: 395-406. https://doi.org/10.1016/j.carbon.2013.09.015
32. Zhu R, Sun Z, Li C, Ramakrishna S, Chiu K, He LJEn. Electrical stimulation affects neural stem cell fate and function in vitro. *Exp Neurol* **2019**; 319: 112963. https://doi.org/10.1016/j.expneurol.2019.112963
33. Makohliso SA, Valentini RF, Aebischer PJJobmr. Magnitude and polarity of a fluoroethylene propylene electret substrate charge influences neurite outgrowth in vitro. *J Biomed Mater Res* **1993**; 27: 1075-85. https://doi.org/10.1002/jbm.820270813
34. Goenka S, Sant V, Sant SJJoCR. Graphene-based nanomaterials for drug delivery and tissue engineering. *J Control Release* **2014**; 173: 75-88. https://doi.org/10.1016/j.jconrel.2013.10.017
35. Qian Y, Zhao X, Han Q, Chen W, Li H, Yuan WJNc. An integrated multi-layer 3D-fabrication of PDA/RGD coated graphene loaded PCL nanoscaffold for peripheral nerve restoration. *Nat Commun.* **2018**; 9: 1-16. https://doi.org/10.1038/s41467-017-02598-7
36. Jannesari M, Akhavan O, Hosseini HRM. Graphene oxide in generation of nanobubbles using controllable microvortices of jet flows. *Carbon* **2018**; 138: 8-17. https://doi.org/10.1016/j.carbon.2018.05.068
37. Sun Y, Liu X, George MN, Park S, Gaihre B, Terzic A, *et al.* Enhanced nerve cell proliferation and differentiation on electrically conductive scaffolds embedded with graphene and carbon nanotubes. *J Biomed Mater Res A*. **2021**; 109: 193-206. https://doi.org/10.1002/jbm.a.37016
38. Guo W, Wang S, Yu X, Qiu J, Li J, Tang W, *et al.* Construction of a 3D rGO–collagen hybrid scaffold for enhancement of the neural differentiation of mesenchymal stem cells. *Nanoscale* **2016**; 8: 1897-904. https://doi.org/10.1039/c5nr06602f
39. Shen J, Yan B, Li T, Long Y, Li N, Ye M. Study on graphene-oxide-based polyacrylamide composite hydrogels. *Compos. Part A Appl. Sci.* **2012**; 43: 1476-81. https://doi.org/10.1016/j.compositesa.2012.04.006
40. Young W. Review of lithium effects on brain and blood. *Cell Transplant* **2009**; 18: 951-75. https://doi.org/10.3727/096368909X471251
41. Cade JF. Lithium salts in the treatment of psychotic excitement. *Med J Aust* **1949**; 2: 349-352. https://doi.org/10.1080/j.1440-1614.1999.06241.x
42. Kim JS, Chang MY, Yu IT, Kim JH, Lee SH, Lee YS, *et al.* Lithium selectively increases neuronal differentiation of hippocampal neural progenitor cells both in vitro and in vivo. *J Neurochem* **2004**;

89: 324-36. https://doi.org/10.1046/j.1471-4159.2004.02329.x
43. Su H, Chu T-H, Wu W. Lithium enhances proliferation and neuronal differentiation of neural progenitor cells in vitro and after transplantation into the adult rat spinal cord. *Exp Neurol* **2007**; 206: 296-307. https://doi.org/10.1016/j.expneurol.2007.05.018
44. Hashimoto R, Senatorov V, Kanai H, Leeds P, Chuang D-M. Lithium stimulates progenitor proliferation in cultured brain neurons. *Neurosci.* **2003**; 117: 55-61. https://doi.org/10.1016/s0306-4522(02)00577-8
45. Huo K, Sun Y, Li H, Du X, Wang X, Karlsson N, *et al.* Lithium reduced neural progenitor apoptosis in the hippocampus and ameliorated functional deficits after irradiation to the immature mouse brain. *Mol Cell Neurosci* **2012**; 51: 32-42. https://doi.org/10.1016/j.mcn.2012.07.002
46. Chen G, Rajkowska G, Du F, Seraji-Bozorgzad N, Manji HK. Enhancement of hippocampal neurogenesis by lithium. *J Neurochem* **2000**; 75: 1729-34. https://doi.org/10.1046/j.1471-4159.2000.0751729.x
47. Su H, Zhang W, Guo J, Guo A, Yuan Q, Wu W. Lithium enhances the neuronal differentiation of neural progenitor cells in vitro and after transplantation into the avulsed ventral horn of adult rats through the secretion of brain-derived neurotrophic factor. *J Neurochem* **2009**; 108: 1385-98. https://doi.org/10.1111/j.1471-4159.2009.05902.x
48. Williams PA, Campbell KT, Silva EA. Alginate hydrogels of varied molecular weight distribution enable sustained release of sphingosine-1-phosphate and promote angiogenesis. *J Biomed Mater Res A* **2018**; 106: 138-46. https://doi.org/10.1002/jbm.a.36217
49. Espona-Noguera A, Ciriza J, Cañibano-Hernández A, Fernandez L, Ochoa I, Del Burgo LS, *et al.* Tunable injectable alginate-based hydrogel for cell therapy in Type 1 Diabetes Mellitus. *Int J Biol Macromol* **2018**; 107: 1261-9. https://doi.org/10.1016/j.ijbiomac.2017.09.103
50. Gupta NV, Shivakumar HJIjoprI. Investigation of swelling behavior and mechanical properties of a pH-sensitive superporous hydrogel composite. *Iran J Pharm Res* **2012**; 11: 481.
51. Cuomo F, Cofelice M, Lopez FJP. Rheological characterization of hydrogels from alginate-based nanodispersion. *Polymers* **2019**; 11: 259. https://doi.org/10.3390/polym11020259
52. Gong CY, Shi S, Dong PW, Zheng XL, Fu SZ, Guo G, *et al.* In vitro drug release behavior from a novel thermosensitive composite hydrogel based on Pluronic f127 and poly (ethylene glycol)-poly (ε-caprolactone)-poly (ethylene glycol) copolymer. *BMC Biotechnol* **2009**; 9: 1-13. https://doi.org/10.1186/1472-6750-9-8
53. Louis SA, Mak CK, Reynolds BA. Methods to culture, differentiate, and characterize neural stem cells from the adult and embryonic mouse central nervous system. *Basic Cell Culture Protocols*: Springer; **2013**. p. 479-506. https://doi.org/10.1007/978-1-62703-128-8_30
54. Huang F, Shen Q, Zhao J. Growth and differentiation of neural stem cells in a three-dimensional collagen gel scaffold. *Neural Regen. Res* **2013**; 8: 313. https://doi.org/10.3969/j.issn.1673-5374.2013.04.003
55. Völker J, Engert J, Völker C, Bieniussa L, Schendzielorz P, Hagen R, *et al.* Isolation and characterization of neural stem cells from the rat inferior colliculus. *Stem Cells Int.* **2019**; 2019: 5831240. https://doi.org/10.1155/2019/5831240
56. Cohen J, Zaleski KL, Nourissat G, Julien TP, Randolph MA, Yaremchuk MJ. Survival of porcine mesenchymal stem cells over the alginate recovered cellular method. *J Biomed Mater Res A* **2011**; 96: 93-9. https://doi.org/10.1002/jbm.a.32961
57. Virumbrales-Muñoz M, Ayuso JM, Lacueva A, Randelovic T, Livingston MK, Beebe DJ, *et al.* Enabling cell recovery from 3D cell culture microfluidic devices for tumour microenvironment biomarker profiling. *Sci Rep* **2019**; 9: 1-14. https://doi.org/10.1186/s12916-015-0278-7
58. Xu H, Zhang L, Bao Y, Yan X, Yin Y, Li Y, *et al.* Preparation and characterization of injectable chitosan–hyaluronic acid hydrogels for nerve growth factor sustained release. *J Bioact Compat Polym* **2017**; 32: 146-62. https://doi.org/10.1177/0883911516662068
59. Toosi S, Naderi-Meshkin H, Kalalinia F, Pievandi MT, Hosseinkhani H, Bahrami AR, *et al.* Long bone mesenchymal stem cells (Lb-MSCs): clinically reliable cells for osteo-diseases. *Cell Tissue Bank* **2017**; 18: 489-500. https://doi.org/10.1007/s10561-017-9652-3
60. Grenache DG, Zhang Z, Wells LE, Santoro SA, Davidson JM, Zutter MM. Wound healing in the α2β1 integrin-deficient mouse: altered keratinocyte biology and dysregulated matrix metalloproteinase expression. *J Invest Dermatol* **2007**; 127: 455-66. https://doi.org/10.1038/sj.jid.5700611
61. Hashemi MS, Esfahani AK, Peymani M, Nejati AS, Ghaedi K, Nasr-Esfahani MH, Baharvand H. Zinc finger protein 521 overexpression increased transcript levels of Fndc5 in mouse embryonic stem cells. *J Biosci* **2016**; 41: 69-76. https://doi.org/10.1007/s12038-015-9578-5
62. Mowla SJ. Neural Transdifferentiation of embryonic like stem cells by lithium chloride. *Pathobiol Res* **2022**; 24: 59-67.
63. Farhadi-Azar M, Ghahremani M, Mahboobifard F, Noroozzadeh M, Yaghmaei P, Tehrani FR. Effects of Rosa damascena on reproductive improvement, metabolic parameters, liver function and insulin-like growth factor-1 gene expression in estradiol valerate induced polycystic ovarian syndrome in Wistar rats. *Biomed J* **2022**; 46: 100538. https://doi.org/10.1016/j.bj.2022.05.003
64. Ostrakhovitch E, Byers J, O'Neil K, Semenikhin OJAob, biophysics. Directed differentiation of embryonic P19 cells and neural stem cells into neural lineage on conducting PEDOT–PEG and ITO glass substrates. *Arch Biochem Biophys* **2012**; 528: 21-31. https://doi.org/10.1016/j.abb.2012.08.006
65. Hupalo EA, Campos JRdR, Parabocz CRB. Efficiency of zinc and calcium ion crosslinking in alginate-coated nitrogen fertilizer. *Orbital Electron J Chem* **2018**; 10: 218-25. https://doi.org/10.17807/orbital.v10i3.1103
66. Belbachir K, Noreen R, Gouspillou G, Petibois C. Collagen types analysis and differentiation by FTIR spectroscopy. *Anal Bioanal Chem* **2009**; 395: 829-37. https://doi.org/10.1007/s00216-009-3019-y
67. Wang Z, Hu S, Wang H. Scale-up preparation and characterization of collagen/sodium alginate blend films. *J. Food Qual.* **2017**; 2017. https://doi.org/10.1155/2017/4954259
68. Zhao W, Qi Y, Wang Y, Xue Y, Xu P, Li Z, *et al.* Morphology and thermal properties of calcium alginate/reduced graphene oxide composites. *Polymers* **2018**; 10: 990. https://doi.org/10.3390/polym10090990
69. Radevych D, Gajdardziska-Josifovska M, Hirschmugl CJ, Weinert M. Interaction of Lithium with a Monolayer of Graphene Monoxide. *J Phys Chem C* **2021**; 125: 11820-7. https://doi.org/10.1021/acs.jpcc.1c01069
70. Eble J, Golbik R, Mann K, Kühn KJTEj. The alpha 1 beta 1 integrin recognition site of the basement membrane collagen molecule [alpha 1 (IV)] 2 alpha 2 (IV). *EMBO J* **1993**; 12: 4795-802. https://doi.org/10.1002/j.1460-2075.1993.tb06168.x
71. Balsam LB, Wagers AJ, Christensen JL, Kofidis T, Weissman IL, Robbins RCJN. Haematopoietic stem cells adopt mature haematopoietic fates in ischaemic myocardium. *Nature* **2004**; 428: 668-73. https://doi.org/10.1038/nature02460
72. Macaya DJ, Hayakawa K, Arai K, Spector MJB. Astrocyte infiltration into injectable collagen-based hydrogels containing FGF-2 to treat spinal cord injury. *Biomaterials* **2013**; 34: 3591-602. https://doi.org/10.1016/j.biomaterials.2012.12.050
73. Aydin T, Gurcan C, Taheri H, Yilmazer AJCB, Translational Medicine V. Graphene based materials in neural tissue regeneration. *Adv Exp Med Biol* **2018**; 3: 129-42. https://doi.org/10.1007/5584_2018_221
74. Zarrintaj P, Zangene E, Manouchehri S, Amirabad LM, Baheiraei N, Hadjighasem MR, *et al.* Conductive biomaterials as nerve conduits: Recent advances and future challenges. *Appl Mater* **2020**; 20: 100784. https://doi.org/10.1016/j.apmt.2020.100784
75. Chen Y-SJB. Effects of electrical stimulation on peripheral nerve regeneration. *BioMedicine* **2011**; 1: 33-6. https://doi.org/10.3390/ma13051063
76. Park JB, Sung D, Park S, Min K-A, Kim KW, Choi Y, *et al.* 3D graphene-cellulose nanofiber hybrid scaffolds for cortical

reconstruction in brain injuries. *2D Mater* **2019**; 6: 045043. https://doi.org/10.1088/2053-1583/ab3889
77. Madan M, Bajaj A, Lewis S, Udupa N, Baig J. In situ forming polymeric drug delivery systems. *Indian J Pharm Sci* **2009**; 71: 242. https://doi.org/10.4103/0250-474X.56015
78. Kong H-J, Lee KY, Mooney DJ. Decoupling the dependence of rheological/mechanical properties of hydrogels from solids concentration. *Polymer* **2002**; 43: 6239-46. https://doi.org/10.1016/S0032-3861(02)00559-1
79. Balgude A, Yu X, Szymanski A, Bellamkonda R. Agarose gel stiffness determines rate of DRG neurite extension in 3D cultures. *Biomaterials* **2001**; 22: 1077-84. https://doi.org/10.1016/S0142-9612(00)00350-1
80. Flanagan LA, Ju Y-E, Marg B, Osterfield M, Janmey PA. Neurite branching on deformable substrates. *Neuroreport* **2002**; 13: 2411. https://doi.org/10.1097/00001756-200212200-00007
81. Prange MT, Margulies SS. Regional, directional, and age-dependent properties of the brain undergoing large deformation. *J. Biomech. Eng.* **2002**; 124: 244-52. https://doi.org/10.1115/1.1449907
82. Hollister SJ. Porous scaffold design for tissue engineering. *Nat Mater* **2005**; 4: 518-24. https://doi.org/10.1038/nmat1421
83. Bozkurt A, Deumens R, Beckmann C, Damink LO, Schügner F, Heschel I, *et al.* In vitro cell alignment obtained with a Schwann cell enriched microstructured nerve guide with longitudinal guidance channels. *Biomaterials* **2009**; 30: 169-79. https://doi.org/10.1016/j.biomaterials.2008.09.017.
84. Zhang Z, Nie S, Chen L. Targeting prion-like protein spreading in neurodegenerative diseases. *Neural Regen Res* **2018**; 13: 1875. https://doi.org/10.4103/1673-5374.239433
85. Jurga M, Dainiak MB, Sarnowska A, Jablonska A, Tripathi A, Plieva FM, *et al.* The performance of laminin-containing cryogel scaffolds in neural tissue regeneration. *Biomaterials* **2011**; 32: 3423-34. https://doi.org/10.1016/j.biomaterials.2011.01.049
86. Cheng H, Huang Y, Yue H, Fan YJSCI. Electrical Stimulation Promotes Stem Cell Neural Differentiation in Tissue Engineering. *Stem Cells Int* **2021**; 2021. https://doi.org/10.1155/2021/6697574
87. Fan B, Guo H, Shi J, Shi C, Jia Y, Wang H, *et al.* Facile one-pot preparation of silver/reduced graphene oxide nanocomposite for cancer photodynamic and photothermal therapy. *J Nanosci Nanotechnol* **2016**; 16: 7049-54. https://doi.org/10.1166/jnn.2016.11327
88. Xie C, Sun H, Wang K, Zheng W, Lu X, Ren F. Graphene oxide nanolayers as nanoparticle anchors on biomaterial surfaces with nanostructures and charge balance for bone regeneration. *J Biomed Mater Res A* **2017**; 105: 1311-23. https://doi.org/10.1002/jbm.a.36010
89. ur Rehman SR, Augustine R, Zahid AA, Ahmed R, Tariq M, Hasan AJIjon. Reduced graphene oxide incorporated GelMA hydrogel promotes angiogenesis for wound healing applications. *Int J Nanomedicine* **2019**; 14: 9603. https://doi.org/10.2147/IJN.S218120
90. Balint R, Cassidy NJ, Cartmell SHJAb. Conductive polymers: Towards a smart biomaterial for tissue engineering. *Acta Biomater* **2014**; 10: 2341-53. https://doi.org/10.1016/j.actbio.2014.02.015
91. Bai RG, Muthoosamy K, Manickam S, Hilal-Alnaqbi A. Graphene-based 3D scaffolds in tissue engineering: fabrication, applications, and future scope in liver tissue engineering. *Int J Nanomedicine* **2019**; 14: 5753. https://doi.org/10.2147/IJN.S192779
92. Kim HJ, Thayer SA. Lithium increases synapse formation between hippocampal neurons by depleting phosphoinositides. *Mol Pharmacol* **2009**; 75: 1021-30. https://doi.org/10.1124/mol.108.052357
93. Dong B-T, Tu G-J, Han Y-X, Chen Y. Lithium enhanced cell proliferation and differentiation of mesenchymal stem cells to neural cells in rat spinal cord. *Int J Clin Exp Pathol* **2015**; 8: 2473.